AJNR

MR-pathologic comparisons of wallerian degeneration in spinal cord injury.

J L Becerra, W R Puckett, E D Hiester, R M Quencer, A E
Marcillo, M J Post and R P Bunge

MR-Pathologic Comparisons of Wallerian Degeneration in Spinal Cord Injury

Jose L. Becerra, William R. Puckett, Erik D. Hiester, Robert M. Quencer, Alexander E. Marcillo, M. Judith Donovan Post, and Richard P. Bunge

PURPOSE: To describe the MR manifestations and temporal course of wallerian degeneration that occurs above and below a spinal cord injury, and to compare the MR findings with postmortem histopathology. **METHOD:** Twenty-four postmortem spinal cords from patients with cervical (n = 14), thoracic (n = 6), and lumbar (n = 4) cord injuries were studied with axial T1- and T2-weighted spin-echo MR imaging. Injury-to-death intervals varied from 8 days to 23 years. The images were examined for alteration of signal above and below the injury site. Histologic studies of these cords with axon, myelin, and connective tissue stains were performed at levels equivalent to the MR sections. Immunohistochemical analysis using antibodies to glial fibrillary acetic protein was also performed on 19 cords. Pathologic-imaging comparisons were made. **RESULTS:** MR images showed increased signal intensity in the dorsal columns above the injury level and in the lateral corticospinal tracts below the injury level in all cases in which cord injury had occurred 7 or more weeks before death. In early postinjury survival times (8 days and 12 days) MR findings were normal; histologically there was early wallerian degeneration in only the dorsal columns at 8 days and in both the lateral and dorsal columns at 12 days. MR showed wallerian degeneration in all cases examined at 7 weeks after injury and thereafter. **CONCLUSIONS:** Wallerian degeneration was demonstrated by histology and MR in all specimens in which the injury-to-death interval was greater than 7 weeks. Recognition of wallerian degeneration on MR allows complete analysis of the injury, explains abnormal MR signals at sites remote from the epicenter of the injury, and may be useful in the future in the timing and planning of therapeutic interventions.

Index terms: Wallerian degeneration; Spinal cord, injuries; Spinal cord, magnetic resonance; Pathology

Wallerian degeneration begins with disintegration of the axon and its myelin sheath after axonal connection with the neuronal cell body has been interrupted (1). It is progressive over a period of weeks to months, followed by an extended period of removal of the breakdown products of the myelinated axons. There is a

substantial difference in the time course of these events in the peripheral and central nervous systems (CNS), with the time of degeneration being much longer in the latter (2). Despite this difference, it appears that the sequence of biochemical events, particularly those associated with breakdown of myelin components, is similar in the two parts of the nervous system. Studies after cerebral infarction indicate that magnetic resonance (MR) of the brain and brain stem can show such changes and have provided some data on the time interval between injury and examination when these changes become detectable (3, 4).

We present a histopathologic study of wallerian degeneration in the major motor and sensory fiber tracts in the spinal cord and compare these with alterations on MR. Our purpose is to determine the location and timing of wallerian

Clinical data on patients with wallerian degeneration

Case	Injury-Death Interval	Clinical Level	Cause of Injury	Degree of Loss of Neurologic Function	Anatomic Assessment of Cord Transection
1	8 d	C-5	GSW	Complete	Incomplete
2	12 d	L-1	GSW	Complete	Incomplete
3	2 wk	T-6	GSW	Complete	Complete
4	2 wk	L-2	GSW	Complete	Complete
5	16 d	C-7	Fall	Complete	Incomplete
6	16 d	C-7	Fall	Complete	Incomplete
7	4 wk	C-2	Fall	Complete	Complete
8	5 wk	C-1	MVA	Complete	Incomplete
9	7 wk	T-5	MVA	Complete	Incomplete
10	4 mo	T-2	MVA	Incomplete	Incomplete
11	4 mo	C-4/C-5	MVA	Incomplete	Incomplete
12	6 mo	C-3	GSW	Complete	Incomplete
13	6 mo	C-4	MVA	Complete	Incomplete
14	1 y	C-2	Fall	Incomplete	Incomplete
15	1 y	C-5/C-6	MVA	Complete	Incomplete
16	1 y	C-5/C-6	MVA	Complete	Incomplete
17	1 y	L-3	Crush	Complete	Complete
18	8.5 y	T-1	GSW	Complete	Complete
19	10 y	C-5	Dive	Incomplete	Incomplete
20	13 y	C-5	MVA	Incomplete	Incomplete
21	18 y	L-2	GSW	Complete	Complete
22	20 y	T-12	GSW	Incomplete	Complete
23	22 y	C-7	MVA	Complete	Incomplete
24	23 y	T-3	GSW	Complete	Complete

Note.—GSW indicates gunshot wound; MVA, motor vehicle accident.

degeneration in the injured cord, to describe how this information is useful in image interpretation, and to indicate how it might be useful in future interventional treatments in patients with spinal cord injury.

Methods

Twenty-four spinal cords were obtained at autopsy from persons who had had spinal cord injury during their lifetime. These were placed immediately in 10% neutral buffered formalin for 2 weeks, after which they were stored in 0.01 mol/L phosphate buffer at 4°C. The time from injury to death was between 8 days and 2 weeks in 4 cases, between 2 weeks and 6 months in 9 cases, and between 1 and 23 years in 11 cases. Fourteen cases had cervical injuries, 6 had thoracic injuries, and 4 had lumbar injuries. The patients' ages at the time of death ranged from 16 to 80 years. Seventeen of the 24 cases had complete loss of neurologic function below the level of the injury on premortem neurologic examination. Anatomically, all cases showed substantial, if not complete, loss of cord tissue at the epicenter of the lesion. The injuries in 9 cases were caused by gunshot wounds and in 15 cases by blunt trauma (Table).

MR studies were obtained on a 1.5-T unit and consisted of sagittal, coronal, and axial spin-echo (2000/80/2 [rep-

etition time/echo time/excitations]) T2-weighted images with a 3-mm section thickness, 12- to 16-cm field of view, and 256 × 256 and/or 512 × 512 matrix. T1 sagittal and axial images (650/20/4) were also obtained. A commercial shoulder coil and an experimental 2-inch surface receive only coil were used. Our analysis of the MR features of wallerian degeneration was based primarily on the axial images to conform to the histopathologic sectioning and to locate more accurately the spinal cord tracts. MR images were reviewed, looking for areas of abnormal signal intensity in the dorsal columns above the injury and in the lateral columns below the injury.

A gross and histologic analysis of the cord was done and always included areas several centimeters above and below the injury, even in those cases in which no abnormal MR signal intensity area was identified. Solochrome-cyanine stain was used to detect myelin and myelin breakdown products in the white matter tracts, Sevier-Munger stain was used to evaluate the status of axons and the presence of debris resulting from axonal breakdown, trichrome stain was used to identify connective tissue components, and a hematoxylin-eosin stain was used to evaluate overall tissue integrity and the status of the neurons.

Immunohistochemical analysis was also performed using an antibody to glial fibrillary acetic protein (GFAP) to identify the changes in astrocytes and their processes in response to axonal degeneration and myelin breakdown. This staining was done by sampling lesioned cords at some distance (several cord segments) from the epicenter of injury. These cord samples were embedded in paraffin and sectioned. The slides were kept on a warmer at 31°C overnight, then cleared of paraffin with xylene, rehydrated through a graded alcohol series, and placed in a phosphate buffer saline (PBS) solution. The sections were then permeabilized using 0.3% triton in PBS for 15 minutes. This solution was removed and replaced with the undiluted antibody (goat antirabbit GFAP, Incstar, Stillwater, Fla) for 60 minutes at room temperature, then washed three times with fresh PBS to remove primary. Most of the slides had one section that was incubated in PBS without any primary for an on-site control. They were then incubated in a secondary antibody (Jackson Immunoresearch West Grove, Pa) with a horseradish peroxidase label for 30 minutes. The secondary label was then developed using 0.05% 3′, 3′ diaminobenzedine-4-HCl combined with 0.3% hydrogen peroxide for 3 to 5 minutes, depending on the rapidity of the development of the brown reaction product. The reaction was stopped by washing with large volumes of PBS. The diaminobenzedine reaction product was further enhanced using 1% aqueous osmium tetroxide for 20 to 25 minutes. The osmium was then removed and the sections were washed with large volumes of PBS. They were then counterstained for cellular components using either 2% cresyl echt violet or a hematoxylin-eosin stain, dehydrated, and coverslipped with Pro-Texx coverslip medium (Fisher, Orlando, Fla). There were no adverse staining results attributable to the length of storage.
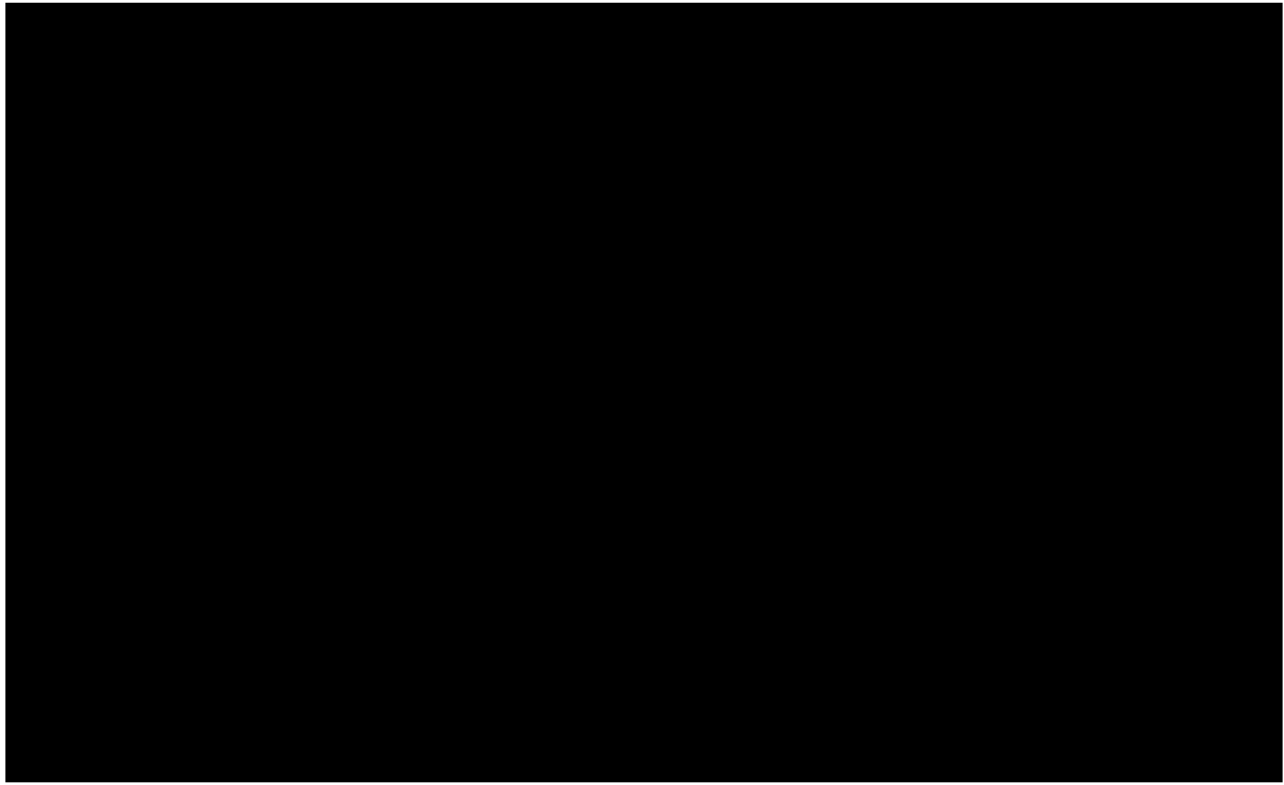
Fig 1. Eight-day survival time after C-5 injury (case 1).

A, Axial T2-weighted spin-echo images (2000/80/2 [repetition time/echo time/excitations], 256 × 256 matrix) at C-1 level shows no area of increased signal intensity in the dorsal columns.

B, Axial T2-weighted images at T-1 level shows no area of increased signal intensity in the lateral columns.

C, High-magnification picture of a silver-stained (Sevier-Munger) section from the dorsal columns above the injury. There is a sharp boundary between the normal axons (*arrowheads*) of the fasciculus cuneatus and the degenerating axons of the fasciculus gracilis (*arrows*).

D, In the corticospinal tract below the lesion, the silver stain showed no evidence of degenerating axons.

Results

Early Postinjury (8 Days to 7 Weeks)

MR evaluation of the eight cases with post-injury survival times of 8 days to 5 weeks (Table) showed no areas of abnormal MR signal intensity in the dorsal columns above the injury site (Fig 1A) or in the corticospinal tracts below the injury site (Fig 1B). Histologic analysis of the case examined at 8 days showed that wallerian degeneration had begun in the dorsal columns above the lesion (Fig 1C), but no abnormality was identified in the lateral columns below the injury (Fig 1D). In the dorsal columns, the axon and myelin breakdown was beginning to be apparent at all cord levels above the lesion, although at this time the myelin breakdown was less advanced than the axon breakdown. There were also many rounded, vacuolated cells (identified primarily

by trichrome staining) that had been activated and had begun phagocytic activity.

Although at 12 days postinjury there were still no MR abnormalities detected in the dorsal or lateral columns remote from the epicenter, histologic analysis showed wallerian degeneration had begun in the lateral columns below the injury. Changes here and in the dorsal columns above the lesion were similar to those seen in the dorsal columns of the 8-day lesion. Between 8 days and 5 weeks, the breakdown of axons and the degeneration of the myelin became more pronounced. GFAP staining to assess astrocyte responses showed no change in this time period.

Late Postinjury (after 7 Weeks)

The initial MR detection of wallerian degeneration was found 7 weeks after injury. At that
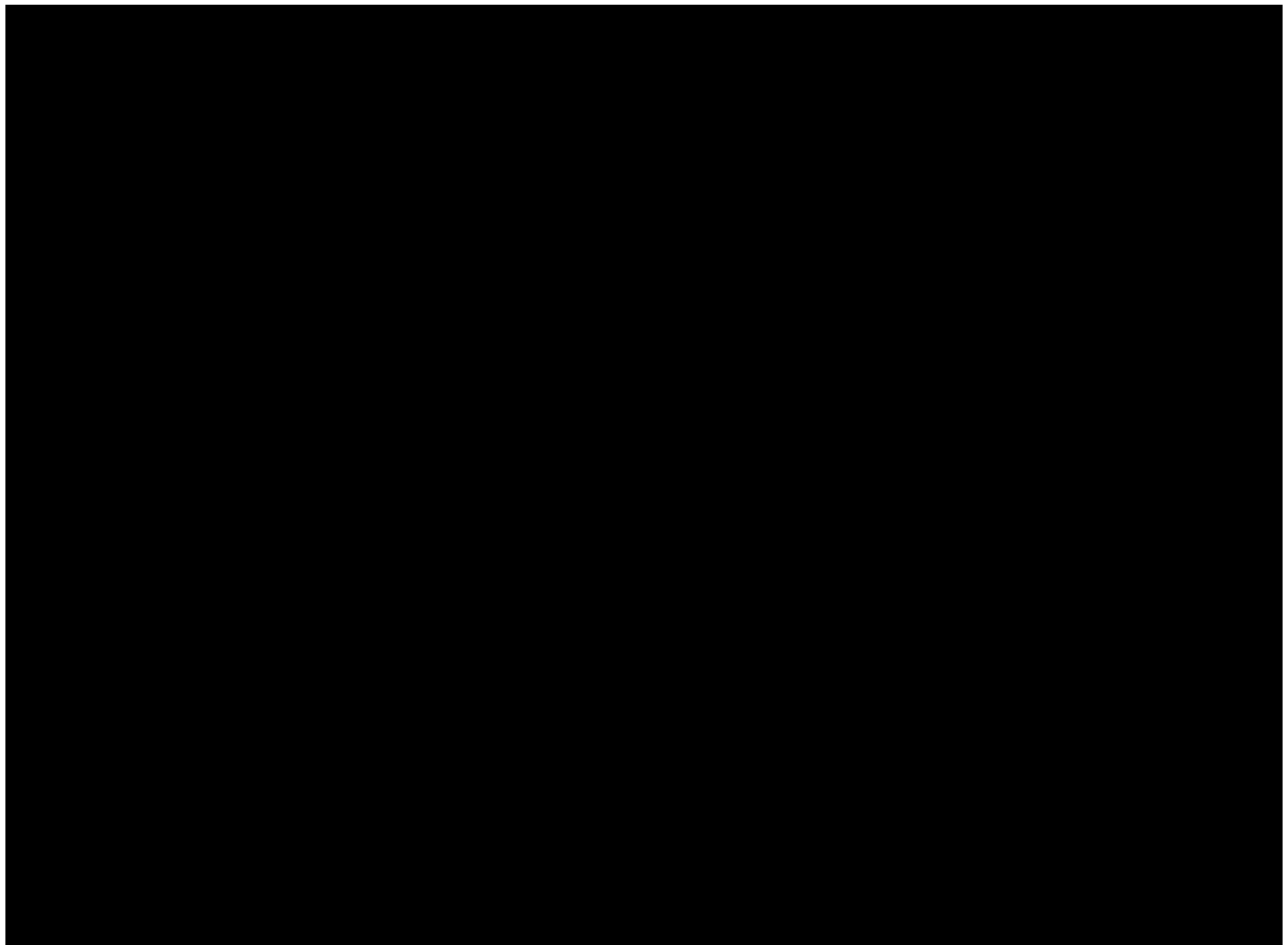
Fig 2. Seven-week survival time after T-5 injury (case 9).

A, Axial T1-weighted images (717/26/2, 256 × 256 matrix) at C-3 show subtle area of increased signal intensity in the dorsal columns (*arrowheads*).

B, Axial T2-weighted image (2300/80/2) at C-3 shows area of increased signal intensity in the dorsal columns (*arrowheads*).

C, In the more medial portions of the dorsal columns (left) above the lesion, there is increased evidence of degeneration with abnormal spacing, loss of axons, and axonal debris throughout the degenerating areas. In the more lateral portions of the dorsal columns (right) the axons are still normal (*arrows*).

D, Axial T2-weighted image (2300/80/2) at L-4 cord level showed area of increased signal intensity in the lateral columns (*arrowheads*).

E, In the corticospinal tracts at L-4 cord level (below the lesion), there is evidence of degeneration characterized by the presence of fragmented axons (*thick arrows*) and swollen axons (thin arrows).

time MR showed areas of increased signal intensity in the dorsal columns above the injury and in the lateral corticospinal tracts below the injury. This area of increased signal intensity was seen in both T1- (Fig 2A) and T2-weighted sequences (Fig 2B). The abnormal signal intensity was identified along the entire length of the affected tract. Histologic analysis showed that the fasciculus gracilis above the lesion site was filled with axonal debris (Fig 2C) containing myelin debris and phagocytic cells, whereas the fasciculus cuneatus was normal. Below the injury level, in the corticospinal tract, axonal de-generation was seen on MR (Fig 2D) and, as above, there was a large amount of myelin and axonal debris (Fig 2E) along with phagocytic cells next to a normal spinocerebellar tract.

In all cases later than 7 weeks, the MR detection of the degeneration was altered only by the increase in definition of the areas of degeneration. The increased signal intensity became more distinct at 6 months after injury (Fig 3A and B). From 7 weeks on, histologic analysis showed an increasing number of phagocytic cells, and by 4 months after injury a clustering of these lipid-laden cells around the blood ves-
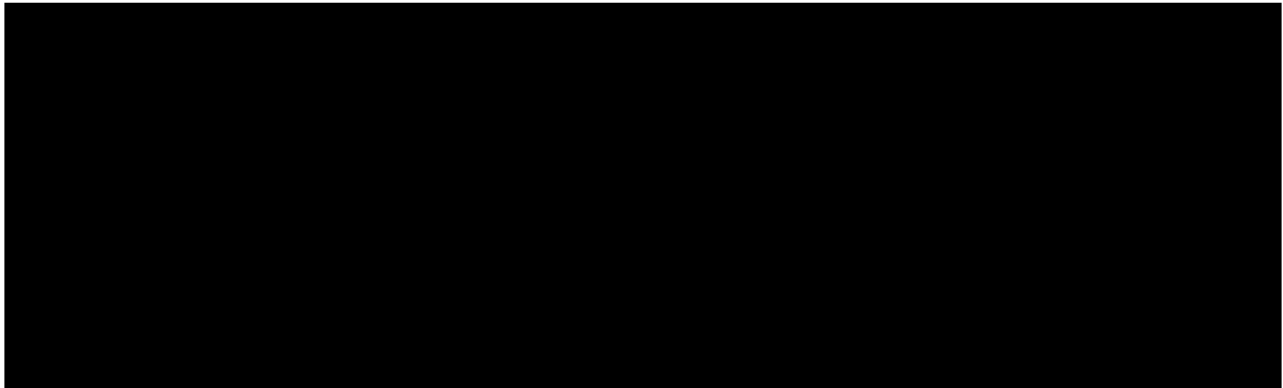
Fig 3. Six-month survival time after C-3 injury (case 12).

A, Axial T2-weighted spin-echo image (2000/80/2, 512 × 512 matrix) at the C-6 level shows areas of increased signal intensity in the lateral columns.

B, Low-magnification picture of a section from this level stained for myelin (solochrome-cyanine) shows that most of the dark blue–staining myelin has been removed from the lateral corticospinal tracts on both sides of the cord.

C, A high-magnification picture of the left corticospinal tract shows that most of the myelin has been lost, and what remains is only distorted myelin debris (*arrows*).

sels was noted. Solochrome-cyanine staining for myelin showed very few myelin debris figures remaining (Fig 3C).

Immunohistochemical studies for the identification of astrocytes using antibodies to GFAP indicated no detectable changes in the condition or distribution of astrocytes and their processes up to 4 months after injury. At 6 months there was a detectable decrease in the intensity of GFAP immunoreactivity of the astrocyte somata and processes and an increase in the size and number of astrocytic processes present in the degenerating areas. Adjacent areas, not undergoing wallerian degeneration, were completely unaffected by these changes, and a sharp boundary existed between the affected and nonaffected areas.

The next time interval available for our study was at 1 year after injury. At this time, there was a continued decrease in the intensity of GFAP staining (as illustrated in Fig 4). With these changes the cell bodies of the astrocytes became indistinguishable from the background of astrocytic processes. There were still many debris-laden cells present.

MR of the specimens harvested between 1 and 20 years after injury showed little change in the areas of wallerian degeneration, although there was a slight intensification of the abnormal signal (Fig 5A). The most notable change in the histology was a completed clean-up of the remaining debris with the astrocytic component becoming dominant (Fig 5B).

Discussion

Wallerian degeneration refers to antegrade degeneration of axons and their accompanying myelin sheaths and results from injury to the proximal portion of the axon or its cell body (3). The precise detection of sites of wallerian degeneration above and below a spinal cord injury can be helpful for understanding the severity of injury at the epicenter of a lesion and its anatomical correlation. If, with MR, we identify wallerian degeneration above the injury, we know that the spinal cord injury caused complete or partial interruption of the ascending axons in the posterior columns. Thus we believe there are compelling reasons to understand how
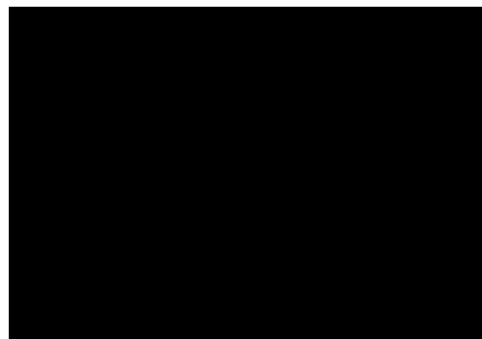

Fig 4. A high-magnification picture of the dorsal columns immunostained for GFAP shows normal staining of the astrocyte somata (*arrowheads*) and processes in the fasciculus cuneatus but diminished immunoreactivity in the degenerated fasciculus gracilis. Here the staining does not distinguish the somata from the background.

A, Axial T2-weighted image (2000/80/2, 256 × 256 matrix) at the C-6 level shows well-defined area of increased signal intensity in the medial aspect of the dorsal columns (*arrowheads*).

B, Low magnification of a section from the corresponding level shows the loss of myelin staining (blue) in the medial portion of the fasciculus gracilis.
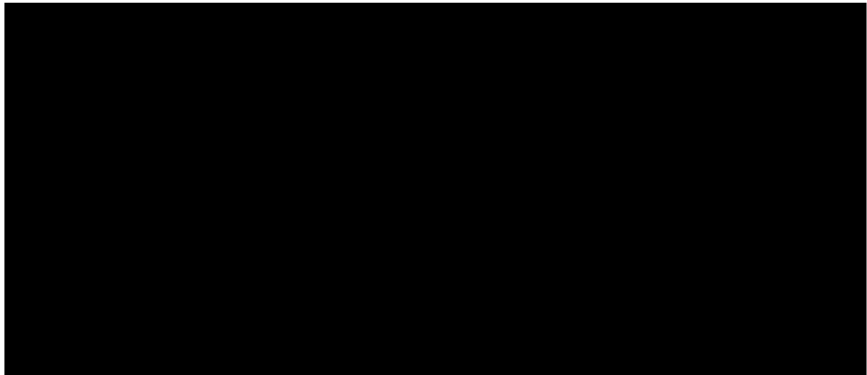
to identify wallerian degeneration in the imaging of the spinal cord injured patient.

In spinal cord injury, one would expect to see wallerian degeneration in the dorsal columns above the lesion and in the corticospinal tracts below the lesion (Fig 6). In the case of a lumbar or thoracic cord injury, the portion of dorsal columns that undergoes wallerian degeneration is smaller than in the case of a cervical injury. This size effect is a function of the number of axons damaged by the injury and the somatotopic arrangement of the ascending fibers in the dorsal column tracts. The corticospinal tract contains fewer axons in distal than proximal regions and therefore becomes smaller in the lumbar region.

The cellular events of wallerian degeneration are different in the central and peripheral nervous systems. These differences in cellular response lead to greatly different rates of debris

Fig 6. Expected major pathways of wallerian degeneration after cord injury.

removal and a dramatically different end result. In the peripheral nervous system, the site of wallerian degeneration in time becomes a terrain conducive to axonal regeneration, whereas in the CNS the end result is a matrix dominated by astrocytes that has failed to accommodate new axonal growth. In a peripheral nerve, axonal breakdown and removal of axonal and myelin debris are accomplished in about 3 weeks (2). In the CNS this process does not begin before 1 week and the removal of axonal debris continues for a period of about 2 years (5–7). Griffin et al (2) suggest that this desultory rate in the CNS results from the fact that central wallerian degeneration does not evoke hematogenous macrophage invasion as it does in the peripheral nervous system. Instead, debris removal must be accomplished by reaction of the resident microglia.

MR imagining of wallerian degeneration in the brain has been described and stages have been proposed (3, 4, 8). Kuhn and colleagues (3) described four stages of wallerian degeneration. In stage 1, there is physical degradation of the axon with little biochemical change in myelin. This occurs during the first 4 weeks and results in no signal intensity abnormality. In stage 2, from 4 to 14 weeks, there is myelin protein breakdown. Myelin lipids remain intact and the tissue becomes more hydrophobic. They proposed that the high lipid-protein ratio results in hypointense signal on T2-weighted MR images. Stage 3, more than 14 weeks, results from subsequent myelin lipid breakdown, gliosis, and changes in water content and structure; the tissue becomes hydrophilic, and there is hyperintense signal on T2-weighted images. Finally, stage 4 occurs several years later and is characterized by volume loss from atrophy. No direct correlations of MR changes with histologic
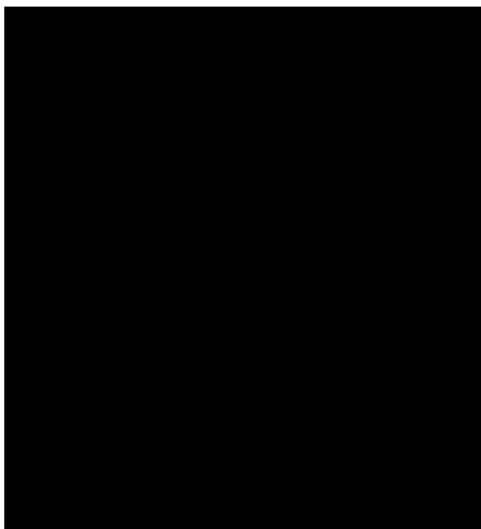
changes of wallerian degeneration in the brain were made in that study.

These changes in signal intensity described by Kuhn et al may be the same in wallerian degeneration of the spinal cord. It is important to remember that the MR signal intensity of the white matter columns in the cord show low signal intensity in T1- and T2-weighted images. This differs from the appearance found in the brain where white matter tracts have higher signal than gray matter on T1-weighted images and lower signal on T2-weighted images (9). Curtin (9) speculated that the low signal of the dorsal and lateral white matter columns on both T1- and T2-weighted images may be caused by the extreme longitudinal organization of ascending and descending myelinated axons in these columns, which may be thought of as analogous to the regular array of collagen fibers in a tendon or ligament. Carvlin (10) noted that the signal intensity for gray and white matter on T1-weighted images depends on the tissue-inherent biophysical parameters of T1, T2, and proton density. In the brain, white matter T1 is so much shorter than that of gray matter that white matter signal intensity exceeds gray matter intensity on T1-weighted images despite the higher gray matter spin density. In the spinal cord, the T1 of gray matter is only slightly shorter than dorsal column white matter and slightly longer than lateral column white matter (10). Therefore, there is very little T1 contrast to be observed and the gray matter–white matter contrast is dominated by the higher spin density of gray matter.

In our series, wallerian degeneration was identified by MR at 7 weeks and longer postinjury survival time. The eight cases with survival times less than 7 weeks (Table) showed no MR abnormality and correspond to stage 1 as proposed by Kuhn et al (3). Histologic findings of the shortest survival time case (8 days) showed early wallerian degeneration in the dorsal column but not in the corticospinal tracts. Degeneration in the corticospinal tracts was first detected histologically at 12 days after injury. This different rate of appearance of wallerian degeneration in ascending and descending tracts has also been identified in spinal cord injuries in the rhesus monkey (11).

The stage at which we first detected wallerian degeneration on MR (7 weeks postinjury survival time) corresponds to stage 2 of Kuhn (4 to 14 weeks) in wallerian degeneration in the brain

(3). At this stage, Kuhn et al found low signal intensity on the T2-weighted images. They theorized that the decreased T2 signal intensity is caused by high lipid-protein ratio as described above. We observed areas of increased signal intensity on T1- and T2-weighted images. The intrinsic characteristics of the white matter of the cord as well as changes in lipid-water ratios may be responsible for the increased MR signal intensity of wallerian degeneration in T1- and T2-weighted images at this early stage. Changes in the tissue at 7 weeks after injury alter the MR image and the signal increases in both T1 and T2 intensity. It is at this time that substantial amounts of cholesterol esters accumulate within the region of wallerian degeneration (5–7). The appearance of cholesterol esters indicates a rapid decrease in intact myelin lipids. It is also during this time that the number of phagocytic cells increases. Our own observations using antibodies to GFAP indicate that a substantial astrocyte alteration does not begin until about 6 months after injury. Therefore, it is during this change in lipid composition and phagocyte activation, and not during the period in which the accrual of GFAC decreases in astrocytes, that the critical first changes in MR signal intensity begin. Because the astrocyte response appears so late in CNS wallerian degeneration (after 6 months), it cannot be implicated in the change in MR image that first appears in CNS tissues at about 7 weeks after injury.

In longer postinjury survival-time cases (stage 3), the MR signal of wallerian degeneration is always of increased signal intensity on T1- and T2-weighted images, and the area of the degeneration becomes better defined (Figs 4A and 5A). Histologically, aside from the described changes in myelin and axons, we see phagocytic cell invasion, which reaches a plateau at 4 to 6 months and begins to decrease after 1 year. Changes (decreased GFAP staining intensity and predominance of the astrocyte processes) in the astrocytes appear at about 6 months, and the matrix continues to be cleared of debris for a period lasting as long as 2 years. Most of the axonal and myelin debris is cleared by 1 year. The number of phagocytic cells begins to drop, and the predominant picture is an astrocytic matrix. Beyond 1 year the phagocytic cells continue to disappear and only a few remain in the long-term survival cases. It is this mostly astrocytic matrix that generates the

Fig 7. Wallerian degeneration in a living pa-
tient 2½ years after C-5 injury.

A, Sagittal gradient-echo T2*-weighted image
(1707/80/2, 70° flip angle) shows prior anterior
fusion from C-3 through C-7.

B, Axial gradient-echo T2*-weighted image
(800/18/20°) at C-2 shows area of increased sig-
nal intensity in the dorsal columns (*arrows*).
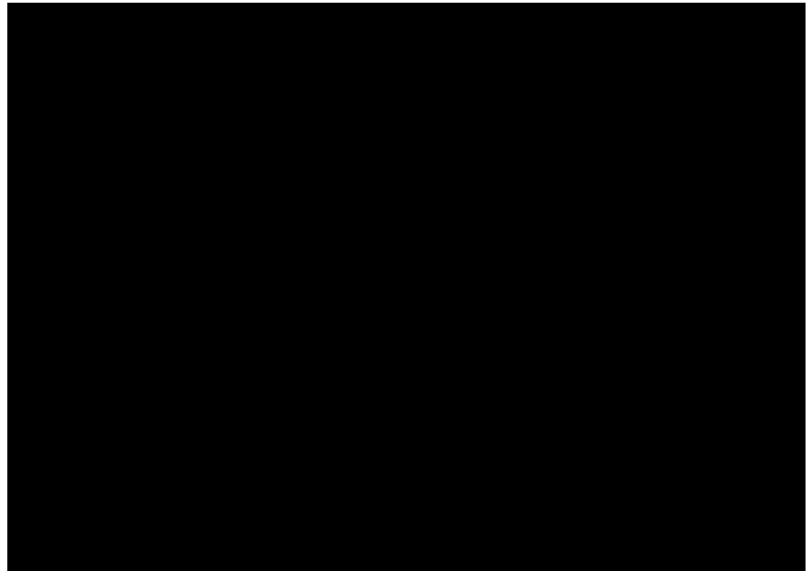
most hyperintense MR signals, associated with
long-term wallerian degeneration. This time
frame corresponds to stage 4 degeneration in
the brain.

These areas of abnormal signal intensity in
the dorsal columns above the injury corre-
sponding to wallerian degeneration can be seen
in the living patient (Fig 7) and should be iden-
tified in routine imaging. Terrae et al (12) have
described the MR appearance of wallerian de-
generation of the injured spinal cord, showing
the areas of increased signal intensity on T2-
weighted images that correspond to wallerian
degeneration in sagittal images. We believe
that the analysis of axial images is much more
revealing, because tract identification is possi-
ble and partial volume-averaging effects are
negated.

Our analysis not only explains abnormal MR
signals at sites remote from the epicenter of
injury but also may be useful in analysis of
events occurring at the lesion epicenter. It may
also provide useful information if therapeutic
intervention is considered, because recent ad-
vances in identification of factors influencing
CNS regeneration suggest the potential use of
neuronal transplantation (13), or Schwann cell
transplantation (14), or the introduction of an-
tiinhibitory factors (15) to improve repair after
spinal cord injury. Understanding the timing of
degeneration of spinal cord tracts will be of im-
portance if such interventions are to be under-
taken.

In summary, we have described the MR signal
intensity changes and the histologic changes

that occur in wallerian degeneration of the cord
after spinal cord injury. The earliest time at
which areas of increased signal intensity on
T1- and T2-weighted images corresponding to
wallerian degeneration can be detected by MR
is 7 weeks in cadaver cords. The stage of hy-
pointense signal on T2-weighted images de-
scribed by Kuhn et al (3, 4) in wallerian de-
generation of the brain was not seen. An
analysis of posttraumatic MR images of the
spinal cord allows a more complete analysis
of the nature and severity of spinal cord le-
sions and may be useful in planning therapeu-
tic interventions in the future.

Acknowledgments

References

1. Waller AV. Experiments on the section of the glossopharyngeal
   and hypoglossal nerves of a frog, and observations of the alter-
   ations produced thereby in the structure of their primitive fiber.
   Philos Trans R Soc Lond Biol 1850;140:423–429
2. Griffin JW, George R, Lobato C, Tyor WR, Yan LC, Glass JD.
   Macrophage responses and myelin clearance during wallerian
   degeneration: relevance to immune-mediated demyelination. *J
   Neuroimmunol* 1992;40:153–166
3. Kuhn MJ, Mikulis DJ, Ayoub DM, Kosofsky BE, Davis KR, Taveras
   JM. wallerian degeneration after cerebral infraction: evaluation
   with sequential MR imaging. *Radiology* 1989;172:179–182

4. Kuhn MJ, Johnson KA, Davis KR. Wallerian degeneration: evaluation with MR imaging. *Radiology* 1988;168:199–202

5. Miklossy M, Van der Loos H. The long-distance effects of brain lesions: visualization of myelinated pathways in the human brain using polarizing and fluorescence microscopy. *J Neuropathol Exp Neurol* 1991;50:1–15

6. Miklossy M, Clarke S, Van der Loos H. The long-distance effects of brain lesions: visualization of axonal pathways and their terminations in the human brain by the Nauta method. *J Neuropathol Exp Neurol* 1991;50:595–614

7. Miklossy J, Van der Loos H. Cholesterol ester crystal in polarized light show pathways in the human brain. *Brain Res* 1987;426:377–380

8. Inoue Y, Matsumura Y, Fukuda T, et al. MR imaging of wallerian degeneration in the brainstem; temporal relationships. *AJNR Am J Neuroradiol* 1990;11:897–902

9. Curtin AJ, Chakeres DW, Bulas R, Boesel CP, Finneran M, Flint E. MR imaging artifacts of the axial internal anatomy of the cervical spinal cord. *AJNR Am J Neuroradiol* 1989;152:835–842

10. Carvlin MJ, Asato R, Hackney DB, Kassab E, Joseph PM. High-resolution MR of the spinal cord in humans and rats. *AJNR Am J Neuroradiol* 1989;10:13–17

11. Bersnahan JC, King JS, Martin GF, Yashon D. A neuroanatomical analysis of spinal cord injury in the rhesus monkey (*Macaca mulatta*). *J Neurol Sci* 1976;28:527–542

12. Terrae S, Taneichi H, Abumi K. MRI of wallerian degeneration of the injured spinal cord. *J Comput Assist Tomogr* 1993;17(5):700–703

13. Normes HO, Moorman SJ, Mihajlov AR, Pulford BE, Whalen LR. Intraspinal transplant of cathecolamine containing cells and fetal spinal cord and iris tissues in the adult rat. *Adv Neurol* 1993;59:185–197

14. Paino CL, Bunge MB. Brief communication: induction of axon growth into schwann cell implants grafted into lesioned adult rat spinal cord. *Exp Neurol* 1991;114:254–257

15. Schnell L, Schwab ME. Axonal regeneration in the rat spinal cord produced by an antibody against myelin associated neurite growth inhibitors. *Nature* 1990;343(6255):269–272
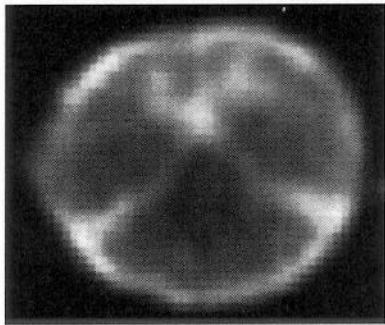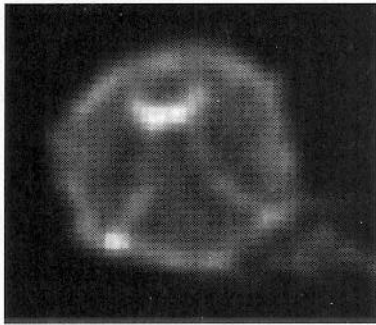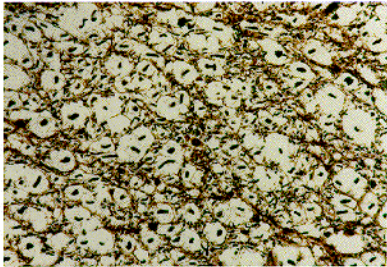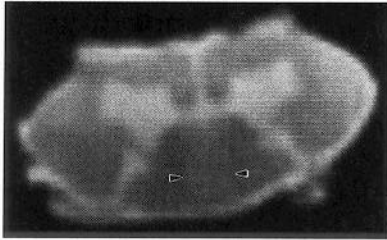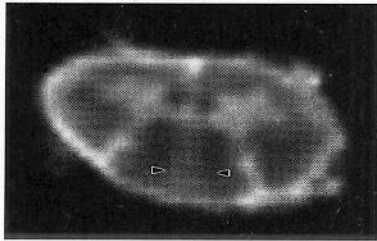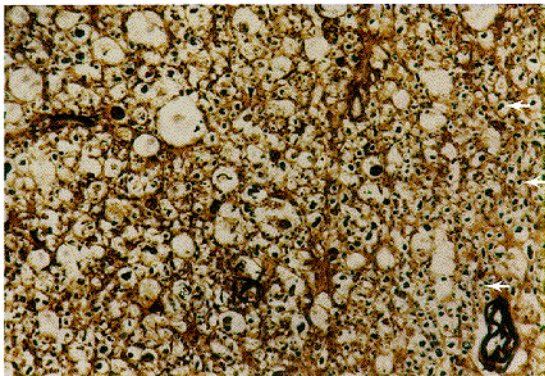
A **B**
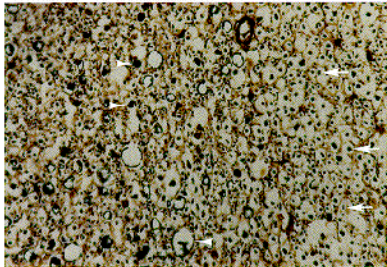
C   D

A   **B**

c
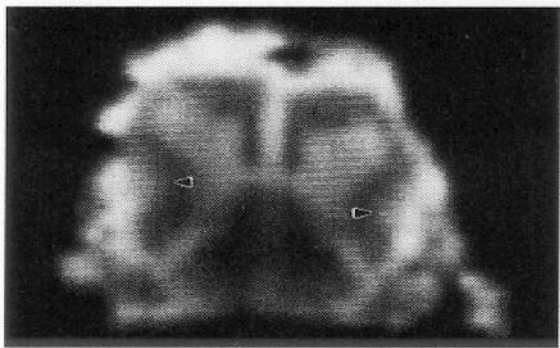
D
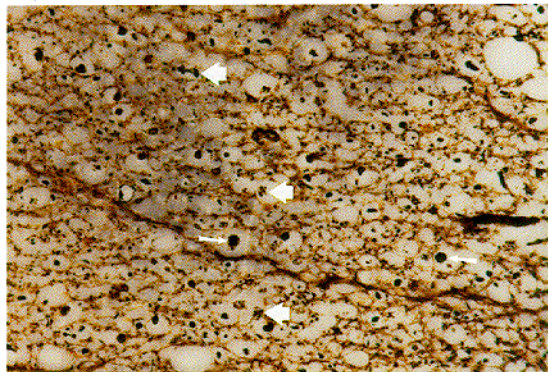
E
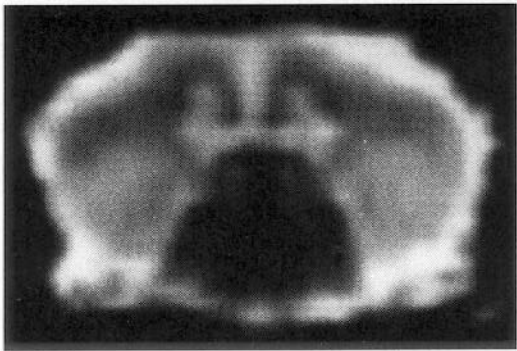
A

B

c

A

B

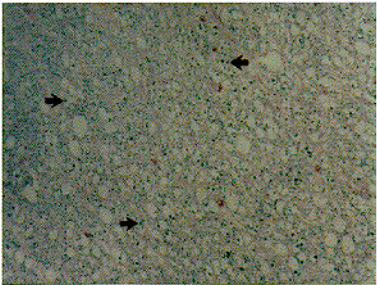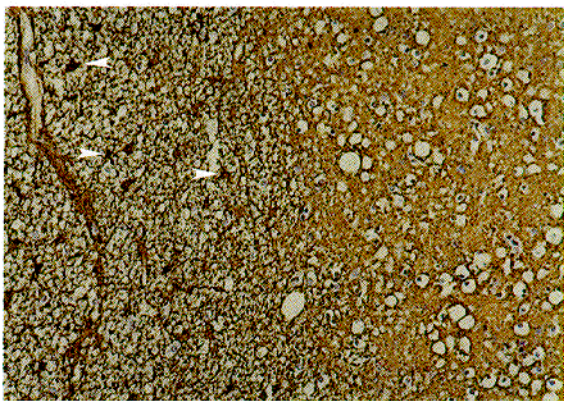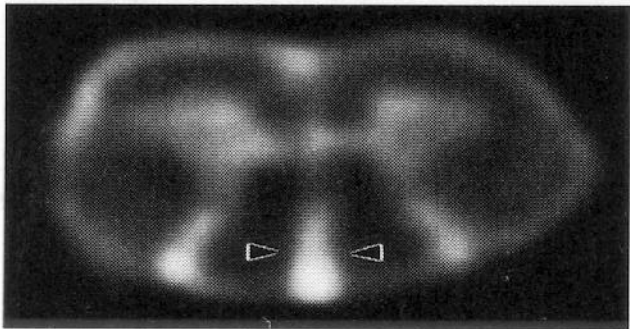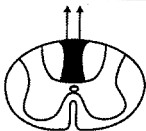A   B

Ascending degeneration

Cord lesion

Descending degeneration